

Antireflection Coatings Using Zinc Oxide Nanostructures

by

Pettigadi Giridhar

A research study submitted in partial fulfillment of the requirements for the
degree of Master of Engineering in
Nanotechnology

Examination Committee: Dr. Gabriel Louis Hornyak (Chairperson)
Dr. Tanujjal Bora
Assoc. Prof. Erik L. J. Bohez

Nationality: Indian
Previous Degree: Bachelor of Technology in
Electronics and Communication Engineering
Jawaharlal Nehru Technological University
Hyderabad, Telangana, India

Scholarship Donor: AIT Fellowship

Asian Institute of Technology
School of Engineering and Technology
Thailand
January 2019

Acknowledgement

I would like to express my profound sincerity towards Dr. Gabriel Louis Hornyak, my advisor for his precious guidance and constant inspiration and feeling of uplifting and the committee member, Dr. Tanujjal Bora for his priceless comments and recommendations for the successful completion of this Research work.

I will be thankful to all members of Nanotechnology department including faculties, senior students and staff, who were very helpful and nurtured me in accomplishment of this research work. I also feel grateful to be a part of the institute which helped me through its excellent facilities, various equipment and great environment to study.

I would also like to thank with my deepest gratitude to my parents and family members for their love, support and valuable encouragement and my friends for supporting me during my stay in AIT.

Abstract

The reflective properties of a surface mainly depend on the surface structure and its roughness. This research is to produce antireflective coatings made with thin film ZnO. But, the ZnO in the coating can be deposited as different shapes (nanorods and nanocones). So, will the change in shape have an impact on the coating? Will it have any effect on the transmission values of the substrate? What will the level of transparency of ZnO coating be and how will it differ with a change in the shape? This is what we are going to test in this work. A coating of ZnO (Zinc Oxide) is deposited on the glass samples by hydrothermal method. Each sample of glass slide is deposited with a different nanostructure (nanorods and nanocones). Then the water contact angle is measured using tensiometer. The characterization is done through Scanning electron microscope (field emission), followed by the investigation of anti-reflective properties of the ZnO coating.

Table of Contents

<i>CHAPT ER</i>	<i>TITLE</i>	<i>PAG E</i>
	Title Page	i
	Acknowledgements	ii
	Abstract	iii
	Table of Contents	iv
	List of Tables	vi
	List of Figures	vii
1.	Introduction	1
1.1.	Background	1
1.2.	Statement of the problem	1
1.3.	Objectives	2
1.4.	Hypothesis	2
1.5.	Scope of Study	2
1.6.	Limitations of the Study	2
2.	Literature Review	3
2.1.	Antireflection Coatings	3
2.2.	Mechanism of ARC's	3
2.2.1.	Interference	3
2.2.2.	Reflection	5
2.2.3.	Refraction	5
2.3.	ARC Made With ZnO	5
2.3.1.	ZnO Nanocones	8
2.3.2.	ZnO Nanorods	10
2.4.	Various Methods to Produce ARC	12
3.	Methodology	16
3.1.	Flow chart	16
3.2.	Glass Slide Cleaning	16
3.3.	Synthesis of ZnO Nanorods	17
3.3.1.	Seeding	17
3.3.2.	Growth of ZnO Nanorods	17

3.4.	Synthesis of ZnO Nanocones Structure	17
3.4.1.	Seeding	17
3.4.2.	Growth of ZnO Nanocones	17
3.5.	Characterization	17
4.	Results and Discussion	19
4.1.	Antireflection Coatings for Different Concentrations	19
4.2.	ZnO Nanorods	20
4.2.1.	Scanning Electron Microscopy(SEM) Results	20
4.2.2.	Transmission Results	23
4.3.	ZnO Nanocones	25
4.3.1.	Scanning Electron Microscopy(SEM) Results	25
4.3.2.	Transmission Results	28
5.	Conclusion	29
6.	References	30

List of Tables

Table	Title	Page no.
2.1	Various methods for the generation of Nanostructures	20

List of Figures

Figure	Title	Page no.
2.1	The resultant wave, when two individual waves blend into each other, is the sum of amplitudes of the individual waves.	3
2.2	Working of an antireflective coating	4
2.3	Phase difference between the two reflected waves	5
2.4	Electrochemical deposition of ZnO thin film at -3V and a deposition time of (a) 5 seconds, (b) 60 seconds and (c) cross section for 60 seconds.	7
2.5	contact angles achieved for different voltages and different deposition times	7
2.6	ARC mechanism: (a) Incident light through single-layered ARC; (b) several interior reflections at micro-scale; (c) light wave interaction at nanoscale; (d) gradient refractive index	8
2.7	Transmittance spectra at normal incident angle to the three surfaces of (1) plain glass (no moth-eye on the surface), with moth-eye structure made of (2) PAK-01 and (3) PAK-02, respectively.	9
2.8	Bare surface (abrupt changes in RI) vs Moth-eye-like surface (smooth change in RI)	9
2.9	Comparison between ARC's and Moth-eye structure (nano GI coating technology).	10
2.10	A thin film of angled nanorods	11
4.1	The different growth concentrations used for the preparation of antireflection coatings of ZnO nanorods: (a) 50mM, (b) 20mM and (c) 2mM.	19
4.2	Images of nanorods grown at a concentration of 0.5mM, obtained from the test results of Scanning Electron Microscopy (SEM): (left) Top view 50k magnification for the growth duration of 10mins, (right) Top view 50k magnification for the growth duration of 20mins	20
4.3	Images of nanorods grown at a concentration of 2mM, obtained from the test results of Scanning Electron Microscopy (SEM): (a) Top view 50k magnification for the growth duration of 10mins, (b) Top view 50k magnification for the growth duration of 20mins, (c) Top view 50k magnification for the growth duration of 60 mins	21
4.4	Graphical representation for Water contact angle obtained at various Growth durations of nanorods grown with a concentration of 0.5mM	22
4.5	Graphical representation for Water contact angle obtained at various Growth durations of Nanorods grown with a concentration of 2 mM	22

4.6	Transmission comparison between plain and coated samples generated for the growth concentration of 0.5mM and at a growth duration of both 10 mins and 20 mins	23
4.7	Transmission comparison between plain and coated samples generated for the growth concentration of 2mM and at a growth duration of 10 mins, 20 mins and 60 mins All the samples depicted in the above graph were produced for growth concentrations of 0.5mM and 2mM at the growth durations of 10 mins, 20 mins and 60 mins	24
4.8	Images of nanocones grown for a growth duration of 30 mins, obtained from the test results of Scanning Electron Microscopy (SEM): (left)Top view 20k magnification, (right) Cross-sectional view 100k magnification	25
4.9	Images of nanocones grown for a growth duration of 60 mins, obtained from the test results of Scanning Electron Microscopy (SEM): (left)Top view 20k magnification, (right) Cross-sectional view 100k magnification	25
4.10	Images of nanocones grown for a growth duration of 180 mins, obtained from the test results of Scanning Electron Microscopy (SEM): (left)Top view 20k magnification, (right) Cross-sectional view 100k magnification	26
4.11	Graphical representation for Average length of Nanocones obtained at various Growth durations	27
4.12	Graphical representation for Water contact angle obtained at various Growth durations of Nanocones	27
4.13	Transmission comparison between plain and coated samples generated at various growth durations	28

CHAPTER 1

INTRODUCTION

1.1 Background

Among the various branches present in science, surface has become one of the major branches which touches each and every aspect of our lives. Surface is important to any material, whether they are the size of stars and planets or as miniscule as nanosized materials. The surface plays a major role in any science and technology that we investigate or devise. The main reason being that the interactions always occur at the surface first. We can determine the surface area of a material depending on its size and geometric shape.

By modifying the surface texture, we could make wonders. A nanotextured glass surface has been found to suppress reflections up to 0.2% over visible as well as infrared wavelengths. The fact that we could suppress the reflection of a surface has lured a lot of researchers to work on it, which has been driven by the interest to fabricate anti-reflective coatings for various applications in our day-to-day lives as well as industrial applications.

Glass is one of the essential materials in our lives and plays a crucial role in our day-to-day lives as it can be used as optical devices such as lens, window, display, etc. Glass is prioritized for every optical application these days due to its transparency. A glass surface reflects up to 4% of its incident light which results in loss of energy. So, many researchers have considered this to be an important aspect to be controlled and researched in many ways verifying many anti-reflection technologies to suppress the reflection in order to minimize the loss of energy. So, in order to suppress the reflection, we need an antireflective coating (ARC), which works at a wide range of wavelengths and incident angles.

This type of transparent glasses could intensify the customer experience of using an electronic device such as the smart phones and televisions. They may become the future of solar panels, mobiles and lasers. These nanotextured antireflective coatings suppress all the losses of reflection. Hence, this type of science can be used to increase the efficiency of solar panels by suppressing all the reflective losses. Several materials were tested to determine the best material for this application and ZnO proved to be one of the best due to its excellent ability of being able to mold itself into various forms of nanostructures.

1.2 Statement of Problem

- Solar power is one of the best sources of renewable energies. But the major drawback lies in its power conversion efficiency. Not all the incident sunlight is converted into electrical energy. Only about 25-30% of solar power is converted into electric power. The rest of the solar power is just going in vain due to the reflective properties of the solar cell. The reflection causes suppression in efficiency for solar cell. A great solution would be to design an anti-reflective coating and deposit on the solar cell which can lower the reflection of the solar panels. In general, we have to modify the surface texture of glass, by growing ZnO nanorods and ZnO nanocones. These ARC's can be produced using various methods. But all the methods are not industrial friendly, and few are expensive. Even the solar cells are very expensive that they can't be replaced every now then. As the time goes on, a lot of dust and other materials get

accumulated on the surface of the solar cell, so the prepared ARC's should be able to cope with such environmental changes.

1.3 Objectives

Objectives of this research are:

- To prepare coatings of ZnO nanorods and nanocones by hydrothermal process on glass substrates
- To investigate the transmission of light through the ZnO modified and unmodified surfaces.
- To investigate the water contact angle on the ZnO modified and unmodified surfaces

1.4 Hypothesis

The main prediction of my research is that, by modifying the surface structure of glass, i.e., by growing ZnO nanostructures on it, the anti-reflective properties of glass can be enhanced.

1.5 Scope of the study

The main aim of this research is to suppress the reflection in glass panels in order to increase the efficiency of solar panels by using an antireflective coating made of ZnO nanostructures. The ZnO ARC is tested upon a glass slide for both transmission and water contact angle. These properties are evaluated for various growth times at which the ZnO ARC has been produced.

1.6 Limitations of the study

- In our research, ZnO nanorods and nanocones growth is limited only on glass substrates.
- Amongst various seeding techniques present, spray coating is the only technique used for the seeding process of preparing the ZnO ARC.
- The research is only limited to the usage of hydrothermal method, due to the fact that other methods are not industrial friendly and are expensive when compared to the hydrothermal method.

CHAPTER 2

LITERATURE REVIEW

2.1 Antireflection Coatings

Solar energy has the power to change the global energy consumption limits. This renewable source of energy, upon taking proper measures and conducting proper research can become the leading source of global power generation. We have already seen that a glass surface can reflect upto 4% of the total incident light. Even in a typical solar panel the reflection of the glass is 4%, despite the photovoltaic device inside and its conversion efficiency, the power generated is minimized by 4% [6]. So, in order to suppress the reflection, we need an antireflective coating (ARC), which works at a wide range of wavelengths and incident angles. The classic type of ARC's usually has a single layer whose thickness is equivalent to one-fourth of the incident wavelength. Their refractive index is the geometric mean of the indices of substrate and environment [7]. Usually a refractive index of $n = 1.23$ is required of an air-glass interface. The drawback for ARC's is that they suppress the reflection only at particular wavelength. This is where the need arises for a coating which is capable to handle anti reflection at a broadband range and which is also omni directional.

2.2 Mechanism of ARC's

The antireflection technique mainly depends upon three parameters: interference, reflection and refraction.

2.2.1 Interference:

Interference is the key parameter of the antireflection concept. We know that, at a particular time two particles cannot stay at the same point in space. But it is the reverse for waves. They can exist together. For instance, if two waves happen to meet at a particular point, they don't collide, they don't smash each other. They simply blend into each other and form a single wave. The resultant wave is the sum of amplitudes of the individual waves.

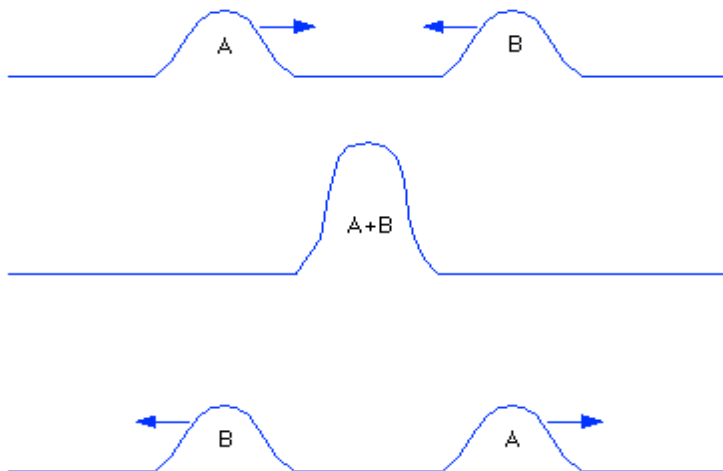


Figure 2.1: The resultant wave, when two individual waves blend into each other, is the sum of amplitudes of the individual waves

Similarly, the objects coated with an antireflective coating have to produce an interference. The antireflective coatings are nothing, but a layer of transparent material coated upon another

kind of transparent object. So, these two layers will have two different refractive indices. When a light wave is incident upon this AR coated object, it gets reflected twice, since it has to pass through two mediums. It is reflected once, when it passes through the first medium, i.e., the AR coating layer and then gets reflected for the second time when it passes through the second medium, the surface of the object. Let us consider the two reflected waves to be R1 and R2. These two waves travel in the same direction as shown in figure 2.2. But these two waves have a phase difference. The main reason being that, R1 is reflected first and then R2 is reflected after travelling an extra distance of $2w$, where w is the width of the antireflective coating. These two waves destruct each other at every point, since they both are different by half the wavelength and result in zero amplitude.

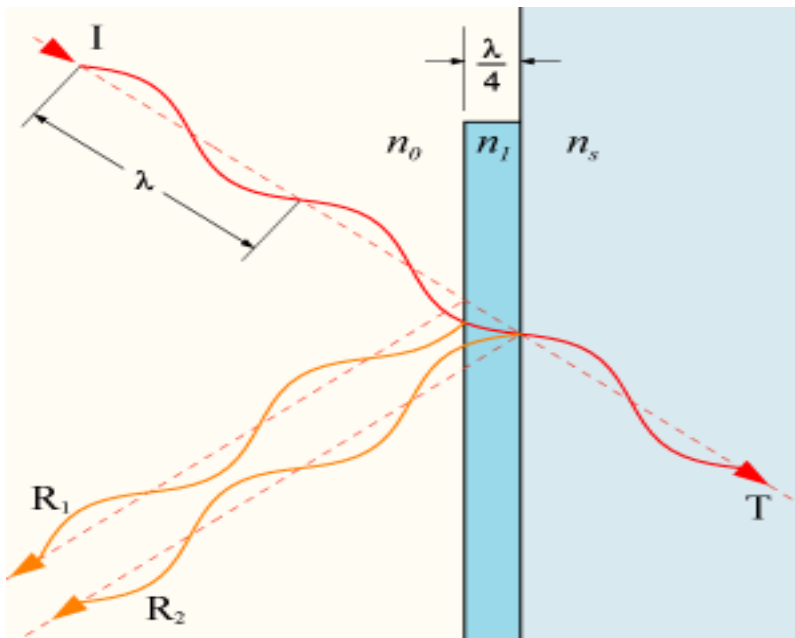


Figure 2.2: Working of an antireflective coating

We have to note that, in order to make the antireflective coatings work, it is very important to produce a phase difference between the two reflected waves. To make this happen, the thickness of the AR coating has to be quarter of the wavelength of light. Then the antireflective coating produces two reflections which interfere destructively with each other.

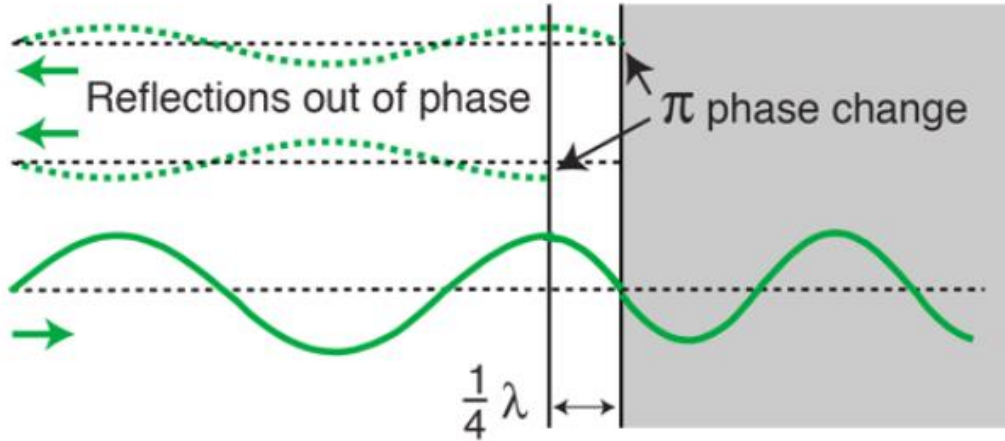


Figure 2.3 Phase difference between the two reflected waves

2.2.2 Reflection

Reflection is a phenomenon which occurs when light travels from one medium to the other. It happens mainly, due to the difference in the refractive indices of the two mediums. While using AR coatings, the light gets reflected twice. For this to happen, the refractive index of the AR coating has to be more than the refractive index of air and less than that of the object upon which we have used the AR coat.

2.2.3 Refraction

Light travels with different speeds, in different mediums. It travels slower in a medium, when compared to its speed in air. We have to consider this point for AR coatings mechanism, since the refractive index and the speed drop go hand-in-hand. It also leads to the shortening of wavelength. This fact is considered for assessing the phase difference between the two reflected waves. The excess distance covered by the second wave should be quarter of the wavelength of light, but not the wavelength of light in air.

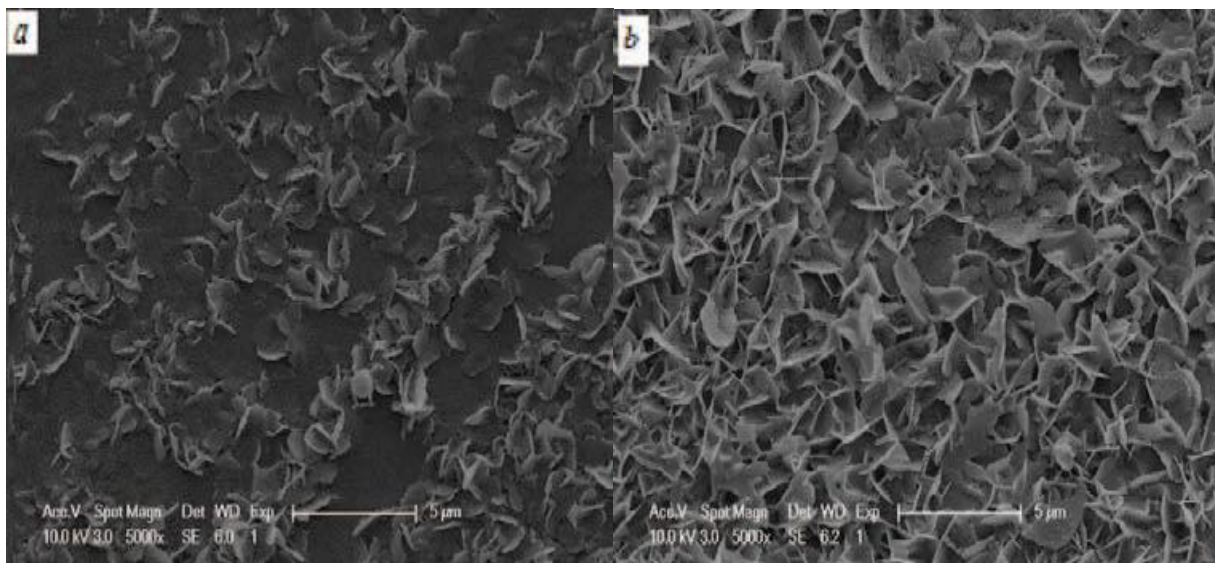
2.3 ARC made with ZnO

Zinc Oxide (ZnO) has been attracting the attention of many researchers for photovoltaic (PV) study and advancement. The promising nature of ZnO has driven to its availability in many applications such as solar cells, optical devices and laser diodes. The appreciable features of ZnO, such as the good refractive index ($n = 1.9$), good transparency in visible region, n-type electrical conductivity (electron mobility $>100 \text{ cm}^2/\text{Vs}$) and wide band gap energy ($E_g = 3.3\text{eV}$) are the main reasons for its usage in solar cells as an anti-reflective coating (ARC) as well as a transparent conductive oxide (TCO). While we use ZnO for solar cells, we have to keep one thing in mind that the roughness of a surface is the key point for transmittance as well as the hydrophobic nature. And as we are mainly concentrating on the transmittance, we can say that a surface with high roughness would cause the incident light to scatter efficiently at the layer above the solar cell resulting in maximizing the optical path length for the light which passes into the system. [44] This would in turn increase the efficiency of the solar cell. But even the roughness has to be in limit. If incase the roughness RMS (Root Mean Square)

reaches up to the value of 150 nm, then the incident light at small wavelengths can get scattered too much, that too with large angles and passes into the ZnO ARC layer and falls prey for unnecessary absorption there. This prevents the light from reaching the absorption layer of the solar cell and hence, decreases the photoelectric conversion rate.

The anti-reflection characteristics of ZnO have been studied in a lot research works. ZnO has also proved to enhance the performance of photovoltaic cells in various instances. The ZnO coatings were observed to not only improve the anti-reflective properties but also demonstrate the ability to avoid or prevent the ultraviolet (UV). [45] The UV region of the solar spectrum has the capability to degrade the organic solar cells at a quick rate and so can suppress the lifespan of a cell. Hence, the UV prevention ability has been an extra advantage particular to increase the lifespan of an organic solar cell. An extra perk would be that the ZnO nanostructures can be grown by hydrothermal method which requires low temperature compared to other methods. This method is also scalable and adaptable with the production of an organic solar cell.

We have already seen that the roughness of a surface plays a major role for its hydrophobic nature and that there are many methods to produce a super-hydrophobic surface. One such method is the electrochemical deposition. We can say that roughness is a factor of both deposit time and voltage. The roughness of a ZnO thin film produced by electrochemical deposition can be increased by increasing the deposition time and the working voltage [2]. The improvement in roughness is nothing but the improvement in hydrophobic behavior of the surface. The below figure 5, depicts three samples of which prepared at -3V. Figure 2.4(a) has a deposition time of 5 seconds while figure 2.4(b) and 2.4(c) (cross section) were deposited for 60 seconds. By analyzing the first two figures i.e. (a) and (b), it can be clearly seen that when the time of deposition for ZnO grain deposit is not long enough, the grain deposited is discrete (on (a)). Which means the surface configuration is smooth While we have look at figure 2.4(b), the grains are linked up to each other and more compactly packed. Which means that as the deposition time is longer the topography of the surface become stronger and the roughness is improved.



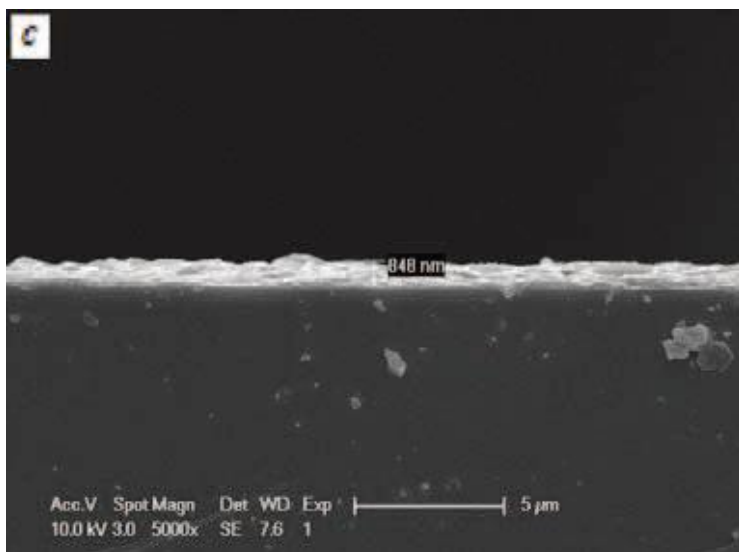


Figure 2.4: Electrochemical deposition of ZnO thin film at -3V and a deposition time of (a) 5 seconds, (b) 60 seconds and (c) cross section for 60 seconds

Source: <https://ieeexplore.ieee.org/document/5667582/>

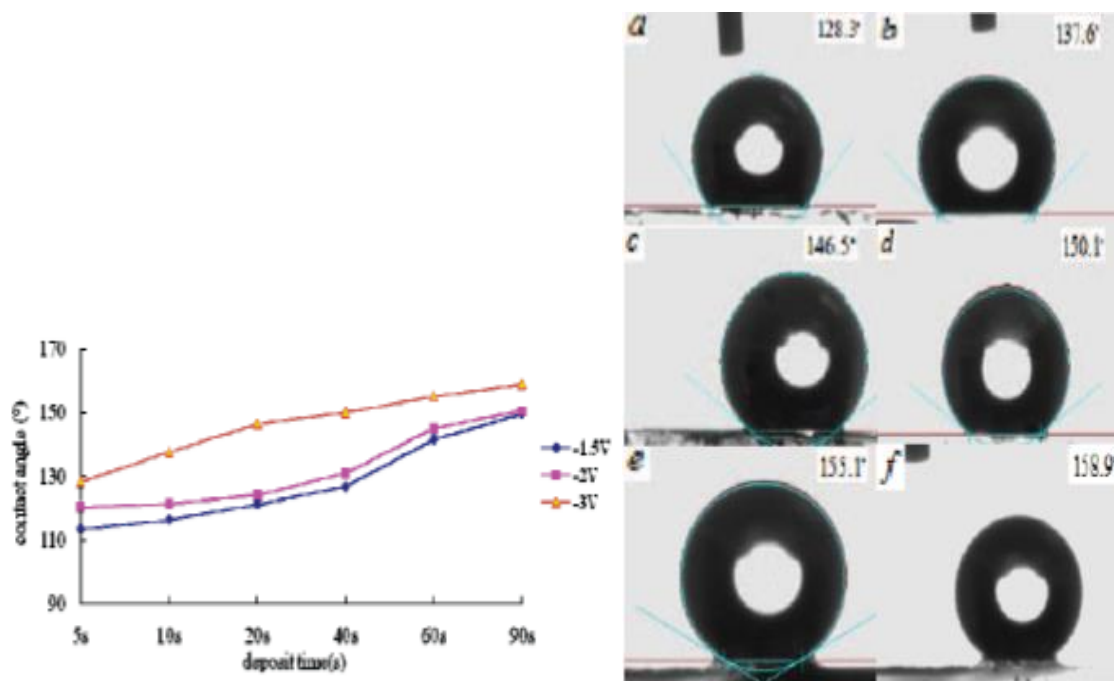


Figure 2.5: contact angles achieved for different voltages and different deposition times

Source: <https://ieeexplore.ieee.org/document/5667582/>

As we can see in the above figure, if the different deposition times and different voltages result in different contact angles. As the deposition time is long enough and the voltage is

sufficiently high, it results in a rough surface. The density in the pores and low surface energy result in a higher contact angle and hence, a super-hydrophobic surface.

2.3.1 ZnO Nanocones

The suppressed reflections due to AR coatings can be achieved by enhanced thickness and refractive index of the AR coat (fig 2.6(a)). They are based mainly on the polarization, wavelength and angle of the incident light. Hence, the AR coatings of single layer can exhibit a better operation for incident light with particular polarization, wavelength and angle.

Whereas, the antireflection coatings built of nanostructures based on moth-eye, exhibit a completely different way of suppressing the reflection. There are two types of interactions between the nano arrays and the incident light, which is based upon the size. When we consider a macrostructure, i.e., when the size of a single unit is being greater than the wavelength, we can expect a usual level of reflection after a partial absorption. The case could be reverse when the gaps and depth between particular units are same level as that of incident light wavelength. Here, the light wave can be absorbed to an extreme level and the reflection can be suppressed. It is due to the fact the light gets caught and results in internal reflections (fig 2.6(b)). The second type (fig 2.6(c) and 2.6(d)) is where the size of each unit is lower than the wavelength of light, or simply nanostructures, the light wave bends gradually as if the AR coat has a gradient refractive index. Even if the light is incident with a different angle, the AR coat welcomes it with the same way. The smooth alteration in refractive index is the same for any incident angle. This way, the reflection is reduced.

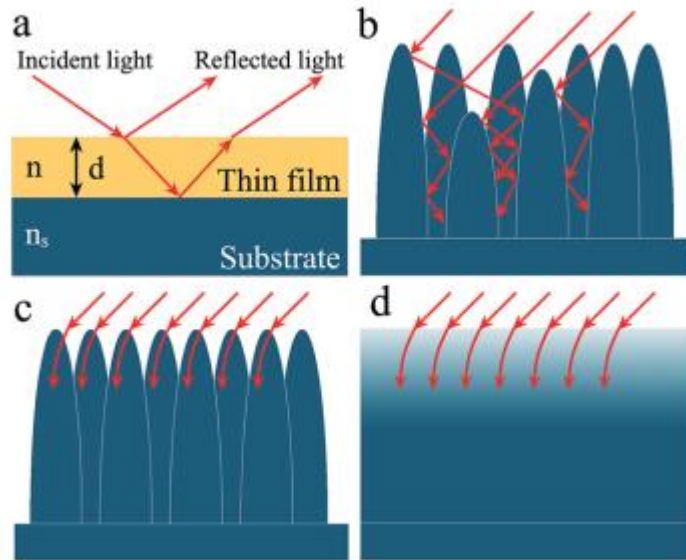


Figure 2.6: ARC mechanism: (a) Incident light through single-layered ARC; (b) several interior reflections at micro-scale; (c) light wave interaction at nanoscale; (d) gradient refractive index

Glass is one of the essential materials in our lives and plays a crucial role in our day-to-day lives as it can be used as optical devices such as lens, window, display, etc. Glass is prioritized for every optical application these days due to its transparency. A glass surface reflects up to 4% of its incident light which results in loss of energy. So, many researchers have considered this to be an important aspect to be controlled and researched in many ways verifying many anti-reflection technologies to suppress the reflection in order to minimize the loss of energy and stray light produced called flare or ghost. This is where we use moth-eye structure for it has an un-parallel antireflection property. This periodic nanoscale structure shows a remarkable performance in suppressing the reflection. The nanoscale tapered pillar array has great antireflection properties for a wide range of wavelengths of incident light and angle. This moth-eye structure when induced on a glass surface increases its transparency from 92% to 96% [5].

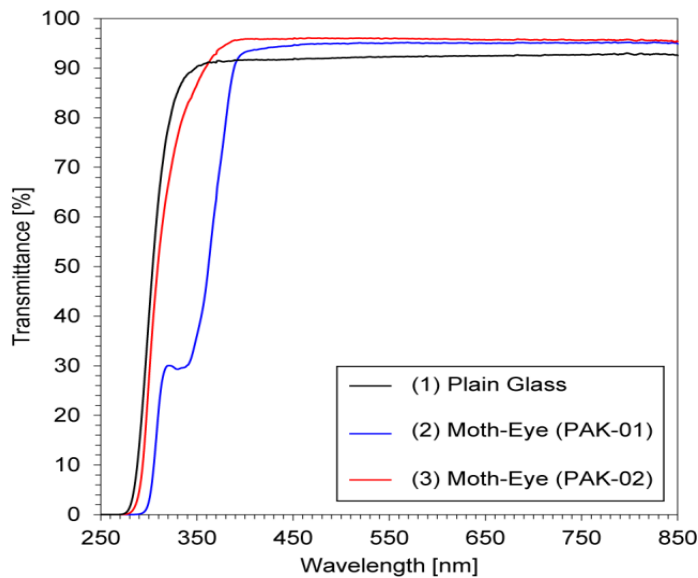


Figure 2.7: Transmittance spectra at normal incident angle to the three surfaces of (1) plain glass (no moth-eye on the surface), with moth-eye structure made of (2) PAK-01 and (3) PAK-02, respectively

Source: <https://ieeexplore.ieee.org/document/7751346/>

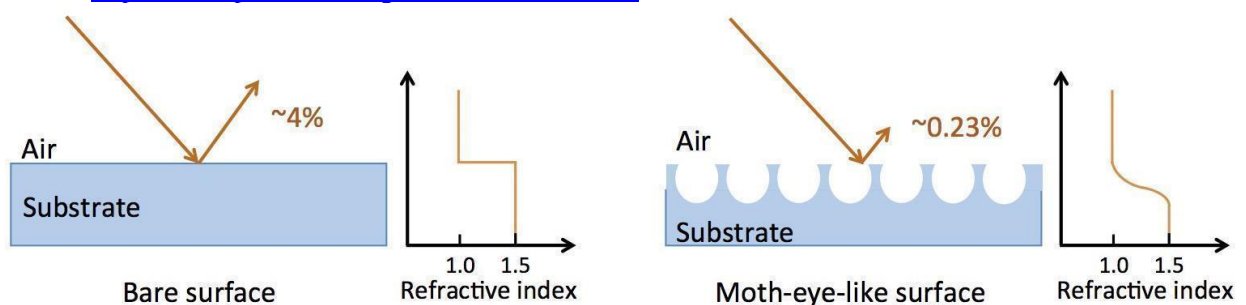


Figure 2.8: Bare surface (abrupt changes in RI) vs Moth-eye-like surface (smooth change in RI)

Solar energy has the power to change the global energy consumption limits. This renewable source of energy, upon taking proper measures and conducting proper research can become the leading source of global power generation. We have already seen that a glass surface can

reflect up to 4% of the total incident light. Even in a typical solar panel the reflection of the glass is 4%, despite the photovoltaic device inside and its conversion efficiency, the power generated is minimized by 4% [6]. So, in order to suppress the reflection, we need an antireflective coating

(ARC), which works at a wide range of wavelengths and incident angles. The classic type of ARC's usually has a single layer whose thickness is equivalent to one-fourth of the incident wavelength. Their refractive index is the geometric mean of the indices of substrate and environment [7]. Usually a refractive index of $n = 1.23$ is required of an air-glass interface. The drawback for ARC's is that they suppress the reflection only at particular wavelength. This is where the need arises for a coating which is capable to handle anti reflection at a broadband range and which is also omni directional. In order to satisfy these conditions a biometric moth-eye was designed [7] - [11]. These moth-eye type structures can be developed by using either top-down or bottom-up approaches. But the coatings derived from top-down approaches can provide 0.10% of reflectance in average whereas bottom-up derived coatings can provide only up to 0.7% [6]. However, top-down is a costly approach in comparison with bottom-up. But indeed, both the surfaces could provide an average reflectance of less than 4% compared to that of an uncoated glass [6].

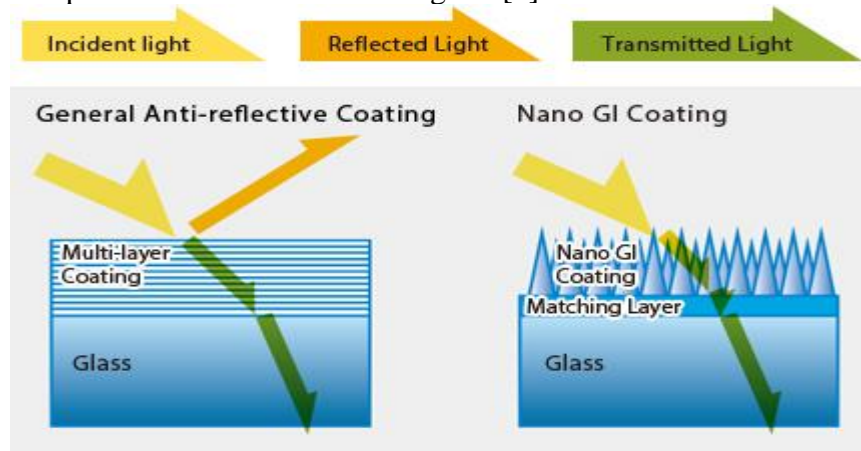


Figure 2.9: Comparison between ARC's and Moth-eye structure (nano GI coating technology)

2.3.2 ZnO Nanorods

Nanorods were used by many researchers to study its effects as an antireflective coat. Many have stated that the refractive index of an antireflective coat has to be in between the refractive indices of air and the object upon which the AR coat was used. Air has a refractive index of 1, which doesn't show any impact on the light wave. Whereas, glass has refractive index of 1.52 and water has around 1.33. These figures do affect the light wave, but not to the extreme level. If we have a look at Silicon, which is the primary material in any solar cell, it has a refractive index of 3.88. So, it undoubtedly reflects up to 30% of the incident light and thus, reducing the power conversion efficiency of a solar cell. The main reason being that the difference between the refractive indices of air and silicon is very high. By depositing a layer of nanorods at an

angle of 45° (as shown in the image below) was observed to achieve a refractive index slightly above to that of air. This means that there are no abrupt changes in the refractive index, and the light doesn't reflect much.

Aerogel is a material; whose structure looks like foam which is completely filled with bubbles. This is a very effective material to suppress the refractive index, but it cannot be mold into thin films. Whereas, the nanorods can be grown to make a very thin layer.

The thin layers made of nanorods will have a similar structure to that of aerogels. Since, the nanorods also possess voids (blank spaces between each other). They are the main reason for achieving a refractive index of just 5% more than that of air. This could impressively enhance the efficiency of solar cells.

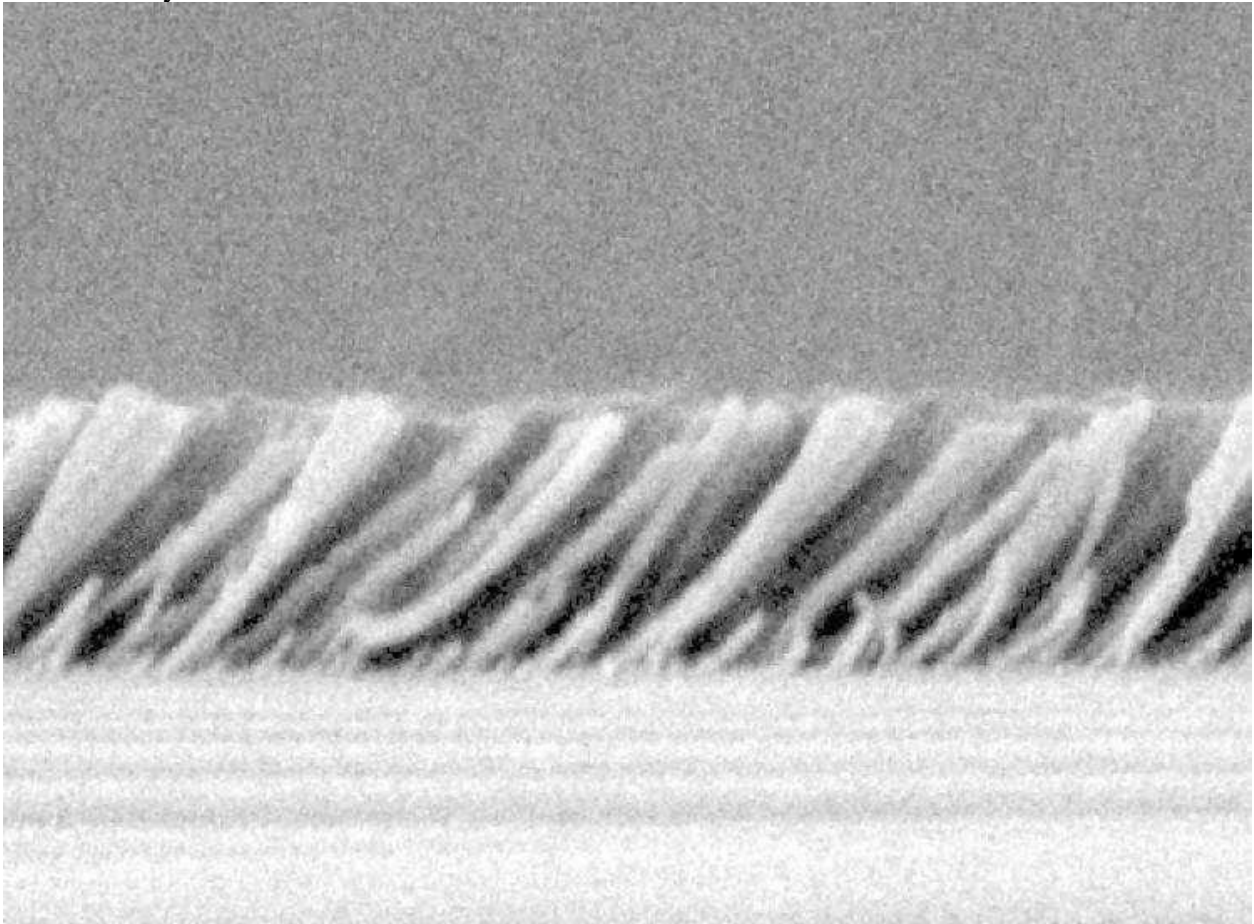


Figure 2.10: A thin film of angled nanorods

Photovoltaics (PV) are the emerging new technologies for producing renewable energies as they can be fabricated easily onto large areas of lightweight substrates at low cost. However, the device has its drawbacks of low efficiency and poor stability [24]. A layer of ZnO nanorods can be deposited to address these problems. When compared with other types of semiconductor nanostructures, ZnO is preferable as it is beneficial in many ways than the

other traditional materials. Among the various advantages of ZnO, achieving One-dimensional structures with high surface areas for light harvesting and direct paths for charge transport are the major ones [25] [26] [27].

As the concentration of the growth solution increases, both the diameter of the ZnO nanorods and the spatial density of the nanorods steadily increases [23]. The transmittance can be increased by varying the growth duration. The highest transmittance of 85% is achieved for the duration of 1h. And it is very well known that by a mild ozone treatment the defect states in ZnO can be passivated which improves the transmittance of ZnO nanorods by 5% over the visible range of 300-800 nm. Mainly, by depositing the ZnO layer followed by UV treatment, the efficiency can be increased from 0.27% - 0.92% [23].

As the growth time increases in addition to the diameter of the nanorods and the spatial density of nanorods, reflectivity of the surface also increases. For the deposition times of 8h, 10, and 12h, the maximum reflectance can be achieved at the growth duration of 12h [28].

ZnO has been gaining much importance these days in the research field due to its wide band gap (3.37 eV) and high electron mobility. Numerous forms of ZnO nanostructures are being prepared every year such as nanospheres, nanoflowers, nanotubes, nanosheets, nanobelts, nanorods, etc.

Few researchers show that nanorods can be prepared by one step hydrothermal process [30]. The research says that the concentration of the growth solution plays a great role in determining the crystallinity of the nanostructures. It is known that, as the reflectance level in visible range grows, the reflectance level in UV region falls stating that the reflectance can be varied by improvising the reagent concentration. It is advised to have grain size in control, as the grain size increases, the reflectance in visible region decreases.

2.4 Various methods to produce ARC

The commendable ARC's receive credit only after a proper making process. Many researchers have used efficient methods for the making of ARC's. One of these methods is the popular hydrothermal method, famous for its low-cost production of thin-layered nanostructures. By using a growth solution of zinc nitrate and HMTA in 1:1 ratio, this method can achieve admirable results. Such as, enhancement in transmission and suppression of reflection. [12] This method operates at a temperature of 95°C. Another inexpensive and time-efficient method used mostly is the spin-coating method. One of the research papers have spin-coated SiO₂ particles and SiO₂ sol, where the particles disperse in the SiO₂ sol without the necessity of any chemical changes and result in suppression of refractive index, which in turn results in the enhancement of transmission. This method helps in providing the ARC's with good mechanical stability and endurance. [16] The next preferable method is the Solvothermal method. This method is advantageous in any many ways. It allows the user to have the power to regulate shape, size and crystallinity of the produced nanostructures. Another plus point is that, it can operate at low temperatures. A research study using solvothermal process of growing TiO₂ nanorods on glass, has achieved impressive results of transmission values up to 80%. [14] And then, the method which comes to mind when we think of scalability is the Bottom-up technique. It is known for its ability to build nanostructures with a low rate of

imperfections. The ZnO nanorods grown upon CuInGaSe₂ [CIGS] solar cell, with a bottom-up technique have proved their performance by suppressing the reflection to nearly 1.46% and enhancing the efficiency of solar cell from 10% to 11.5%. [13]

Table 2.1: Various methods for the generation of Nanostructures

S.no:	Method	Material	Thickness	Contact Angle	Transparency/Reflectance	Reference												
1.	Hydrothermal Method	ZnO+ solution of Zn (NO ₃) ₂ . 6H ₂ O and HMTA in the ratio of 1:1 on Si base	20 nm (at the rate of 10 nm/min)		a) Absorption increases and reflectance decreases at UV region. b) Superhydrophilic surface. c) Etching time increases, reflectance decreases (for every 10 min increase in the etching time, the reflectance decreases by 20% when compared to the previous sample).	[12]												
2.	Bottom-up	ZnO on CuInGa Se ₂ [CIGS] solar cell	100 nm		<div>a) Reflectance decreases from 6.14% to 1.46%. b) Efficiency of solar cell increased from 10% to 11.5%.</div> <table><tr><td></td><td>Reflectance(%)</td><td>Efficiency(%)</td></tr><tr><td>Bare CIGS</td><td>6.14</td><td>10</td></tr><tr><td>Flat ZnO NR AR coating</td><td>2.58</td><td>10.9</td></tr><tr><td>Conical ZnO NR AR coating</td><td>1.46</td><td>11.5</td></tr></table>		Reflectance(%)	Efficiency(%)	Bare CIGS	6.14	10	Flat ZnO NR AR coating	2.58	10.9	Conical ZnO NR AR coating	1.46	11.5	[13]
	Reflectance(%)	Efficiency(%)																
Bare CIGS	6.14	10																
Flat ZnO NR AR coating	2.58	10.9																
Conical ZnO NR AR coating	1.46	11.5																

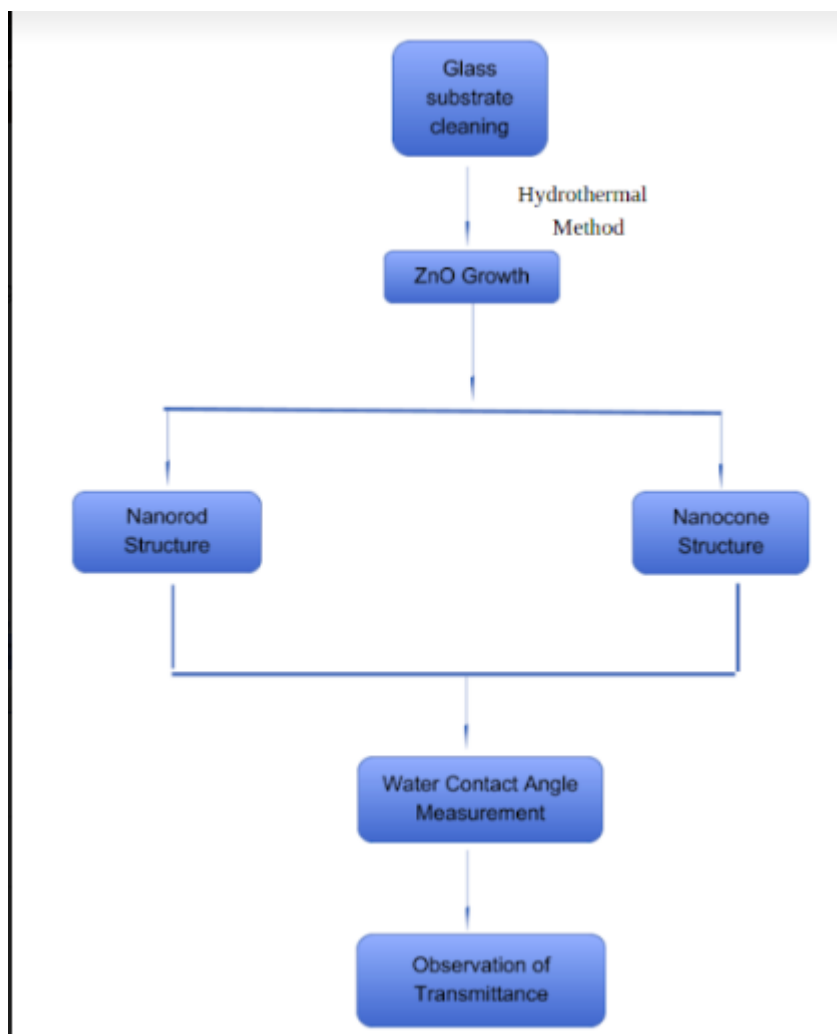
3.	Solvothe rmal process	TiO ₂		90°	Exhibits highest transmittance of 70-80% at 520-800 nm range (bare glass-90%) and negligible absorption in visible region.	[14]
4.	Spin coating	SiO ₂ and SiO ₂ sol			Transmittance is enhanced from 91% to 96-99% which demonstrates that the loss of light is low.	[16]
5.	Nano Imprintin g	Silicon elastom er			Plain surface-92% PDMS-made MOTH EYE-94.3% Vitrified SiO ₂ -95.5% [visible range -470-700 nm]	[1]
6.	Nanoimp rinting Lithograp hy	UV curable resin Inorgani c: glass Organic : polycar bonate			96% [365-750 nm]	[2]
7.	Top- down and bottom- up approach [reactive ion etching (RIE)and wet etching]	Silica nanopa rticles			Top-down: Avg.reflection-0.10% Bottom-up: Avg.reflection-0.69% [Both less than 4% of uncoated glass]	[4]
8.	Nano Imprintin g	UV curable resin			Reflection is lowered to around 5.3%[at 400 nm wavelength total conversion efficiency of GaAs cell was changed from 27.7% to 28.69%]	[6]

9.	Physical vapour deposition (PVD)	TiAlN and TiO ₂			Reflectance suppressed by 3%	[7]
10.	Plasma etching process	Silicon nitride			Avg.reflectance suppressed to below 1% across the spectral range of 300-1200 nm	[8]
11.	Roll to Roll NIL	Aluminium oxide (AAO) SWS on PET substrate. SWS-subwavelength structure PET-polyethylene terephthalate			Transmission of 92% was observed at (visible region) transmittance is increased by 3% reflectance reduced from 5.3% to 0.09%	[9]
12.	Plasma etching process	GaAs Nanograting			Absorption enhanced 98%-100% (at $\lambda=240-873$ nm) and 98%-72% at ($\lambda=873-2400$ nm) for Nanograting GaAs of length ≈ 200 nm	[10]

CHAPTER 3 METHODOLOGY

3.1 Flowchart

The steps involved in my research are depicted in the following flowchart:



3.2 Glass slide cleaning

The cleaning process includes different steps to remove the impurities at the glass slide. It includes three steps within the ultrasonic bath. First, put the glass slides in the soap water for 15 mins and then clean it with DI water after which put them inside the acetone solution maintain it for 15 mins after which finally keep them within the DI water for 15 mins. This process takes around 45 mins to clean the slides and then put the cleaned slides into the oven at the temperature of 100°C and go away it for 20 mins.

3.3 Synthesis of ZnO nanorods

Zinc oxide nanostructures are developed by using Hydrothermal method. This is one of the most used simple method for the synthesis of ZnO nanorods, due the low cost of the experiment process and environmentally friendly and required low temperatures. In hydrothermal method ZnO nanorods are developed on the glass substrate. This process involves two steps:

- ZnO nanoparticle seeding
- Growth of ZnO seeds to nanorods

3.3.1 Seeding

The ZnO seed solution was made by mixing zinc acetate dihydrate [$\text{Zn}(\text{O}_2\text{CCH}_3)_2 \cdot 2\text{H}_2\text{O}$] and pure ethanol. The prepared seeding solution is then to be sonicated for 15 mins. Then finally the glass slide is placed on a hot plate and the seeding solution deposited by spray-coating on to the glass slide.

3.3.2 Growth of ZnO nanorods

A solution of Zinc nitrate hexahydrate [$\text{Zn}(\text{NO}_3)_2 \cdot 6\text{H}_2\text{O}$], hexamethylenetetramine [$(\text{CH}_2)_6\text{N}_4$] and DI water must be used for the growth of Nanorods. In this growth solution, our sample glass slide is dipped horizontally and then placed in the oven at 90°C . After the hydrothermal growth, the glass slide must be cleaned using DI water and left for drying. ZnO nanorods will be formed.

3.4 Synthesis of ZnO Nanocone structure

3.4.1. Seeding

The ZnO seed solution was made by mixing zinc acetate dihydrate [$\text{Zn}(\text{O}_2\text{CCH}_3)_2 \cdot 2\text{H}_2\text{O}$] and pure ethanol. The prepared seeding solution is then to be sonicated for 15 mins. Then finally the glass slide is placed on a hot plate and the seeding solution deposited by spray-coating on to the glass slide.

3.4.2 Growth of ZnO Nanocones

A solution of Zinc nitrate hexahydrate [$\text{Zn}(\text{NO}_3)_2 \cdot 6\text{H}_2\text{O}$], hexamethylenetetramine [$(\text{CH}_2)_6\text{N}_4$], Urea [$\text{CH}_4\text{N}_2\text{O}$] and DI water must be used for the growth of Nanocones. In this growth solution, our sample glass slide is dipped horizontally and then placed in the oven at 90°C . After the hydrothermal growth, the glass slide must be cleaned using DI water and left for drying. ZnO nanocones will be formed.

3.5 Characterization

The architecture of the ZnO films prepared by the above method must be characterized by field emission scanning electronic microscopy (FESEM). The optical properties such as transmittance and absorbance will be observed by using an UV-vis spectrometer which covers the spectral regions from 300nm to 800nm. In order to measure the contact angle, we use Dynamic/Static Optical Contact Angle Meter / Interfacial Tensiometer. The machine consists of an optical table placed to support all the instruments except the camera. The table is to provide well flatness and good vibration isolation. The machine then consists of a solid surface sample fixed with the help of a 3D manipulator and also consists of a micro-syringe

mounted above the test sample in order to produce a water droplet. One end of the machine consists of an LED light source which illuminates the water droplet in order to improve the image quality. The other end of the machine has a digital camera for capturing the image of the water droplet. We accomplish the CA measurement by dropping a 2 μ l of water droplet at 10 different positions on the ZnO film. Then a CCD camera captures the static images in order to measure the water contact angle.

CHAPTER 4

RESULTS AND DISCUSSIONS

4.1 Antireflection coatings for different concentrations:

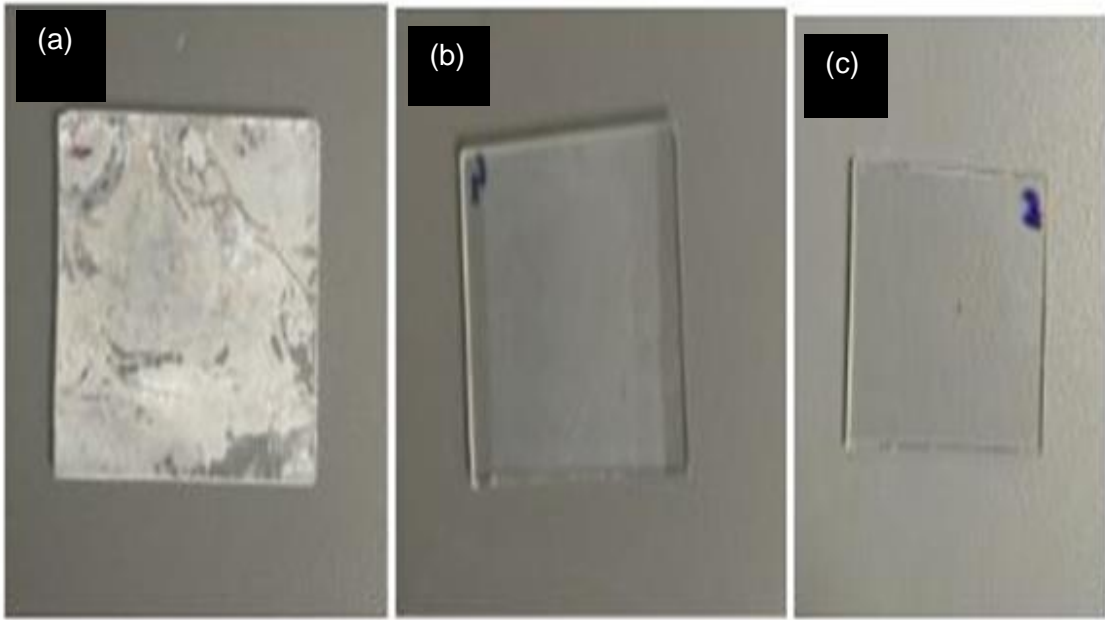


Figure 4.1: The different growth concentrations used for the preparation of antireflection coatings of ZnO nanorods: (a) 50mM, (b) 20mM and (c) 2mM

In image (a), the sample with 50mM concentration is observed to have a white layer formed upon it, leaving the glass sample not transparent anymore. The same with image (b), a white layer is formed, but not as much thick as the image in (a). The transmission values are lower than that of the plain glass for both 50mM and 20mM concentrations. Then finally, the sample with a concentration of 2mM has been observed to be transparent, without any white layer on it. Even the transmission values for this sample are better than that of the plain glass, leaving this sample to be the best sample so far. This sample has achieved the desired transmission values for our prepared antireflection coating.

4.2 ZnO Nanorods:

4.2.1 Scanning Electron Microscopy (SEM) Results:

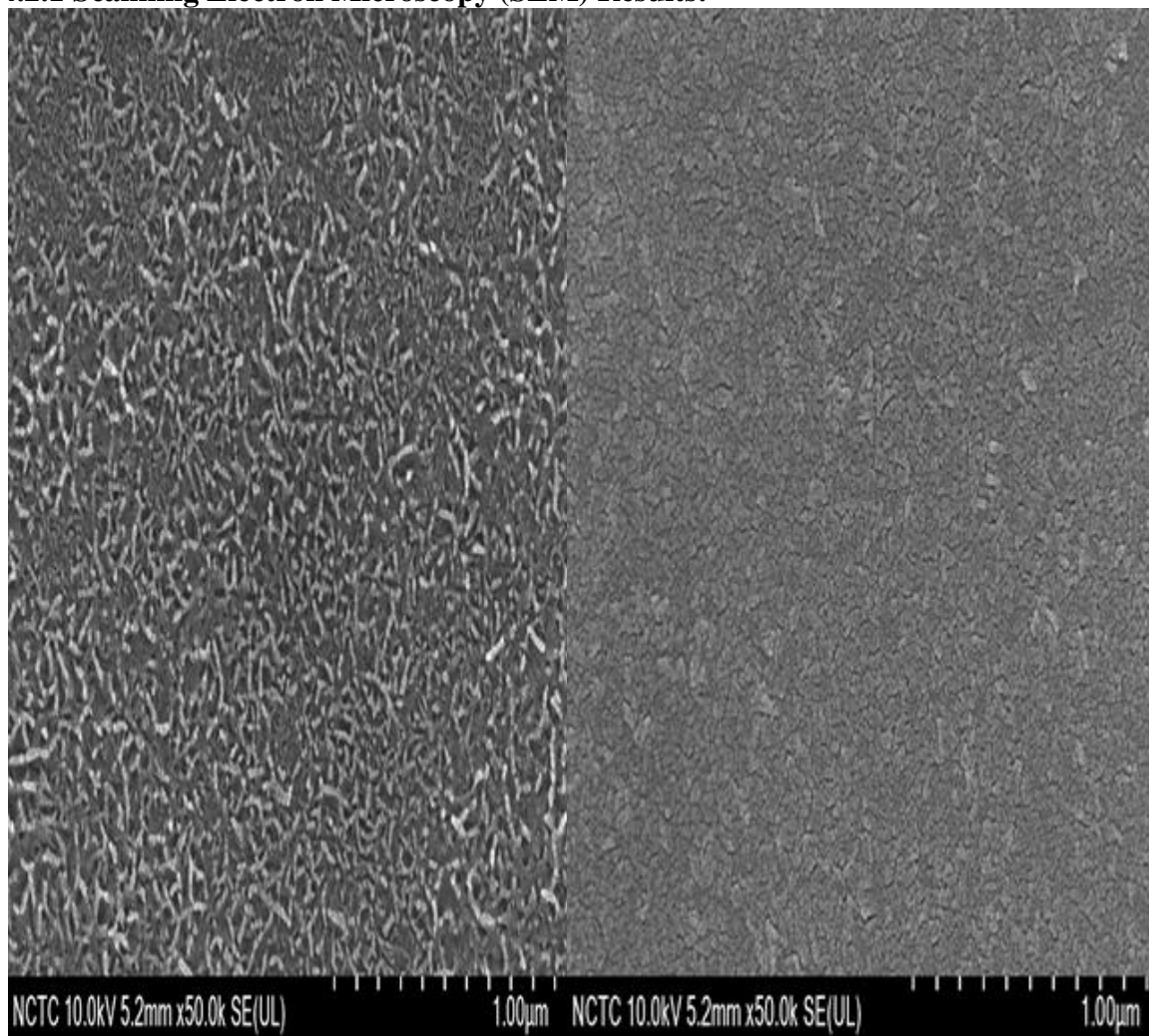


Figure 4.2: Images of nanorods grown at a concentration of 0.5mM, obtained from the test results of Scanning Electron Microscopy (SEM): (left) Top view 50k magnification for the growth duration of 10mins, (right) Top view 50k magnification for the growth duration of 20mins

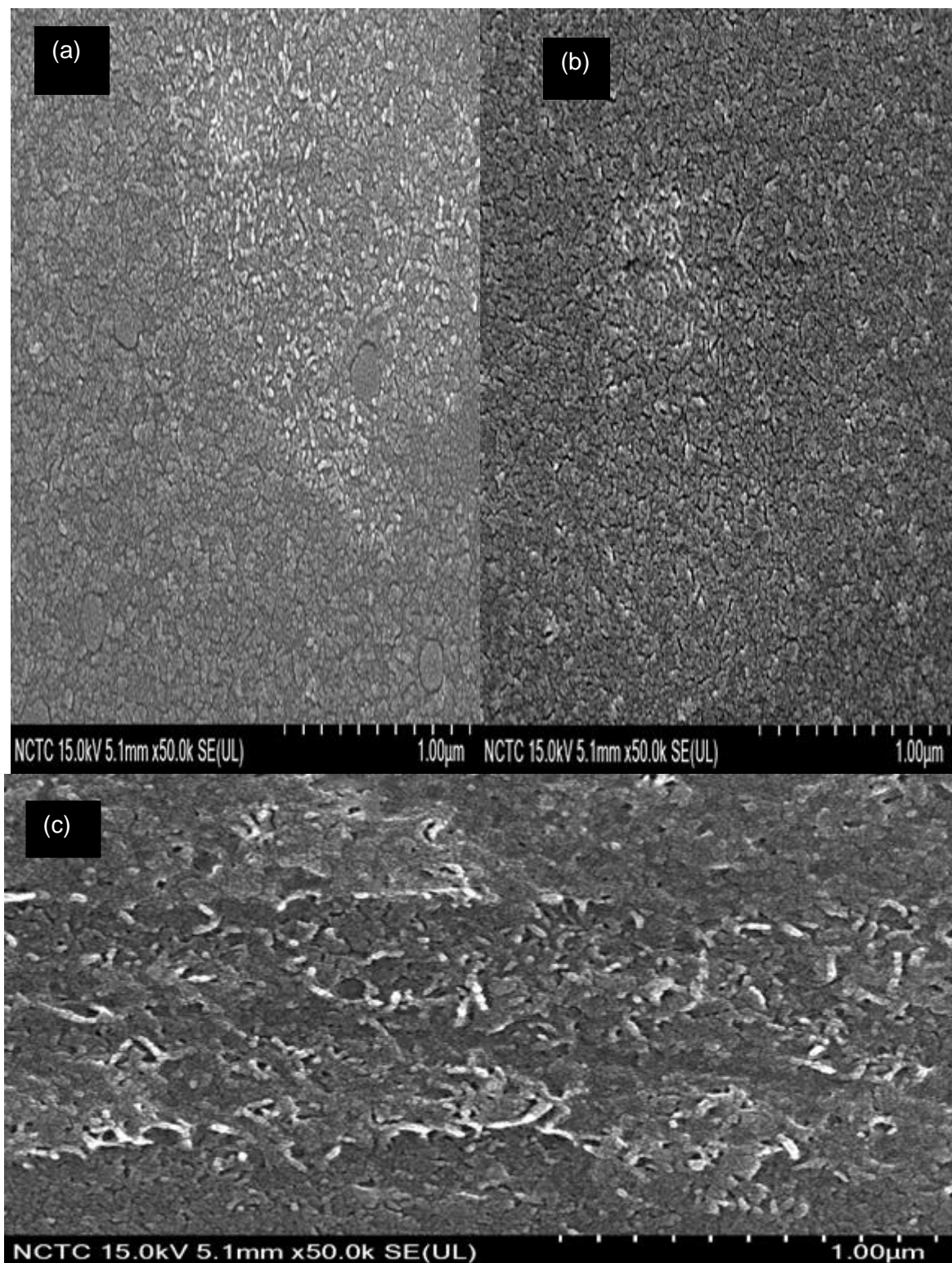


Figure 4.3: Images of nanorods grown at a concentration of 2mM, obtained from the test results of Scanning Electron Microscopy (SEM): (a) Top view 50k magnification for the growth duration of 10mins, (b) Top view 50k magnification for the growth duration of 20mins, (c) Top view 50k magnification for the growth duration of 60 mins

The above images from figure 4.2 and figure 4.3 depict the images of SEM test for the generated Anti-reflective coating of nanorods for different growth durations of 10 mins, 20 mins and 60 mins, as well as different growth concentrations (0.5mM and 2mM). For the both the concentrations, as the growth duration increases, the surface roughness has been observed to be steadily increasing. The nanorods have spread across the sample surface without much gaps in the between, resulting in good surface roughness. The size of the nanorods can be observed to be steadily increasing. The gaps between the nanorods were also lessening as the growth duration was increased.

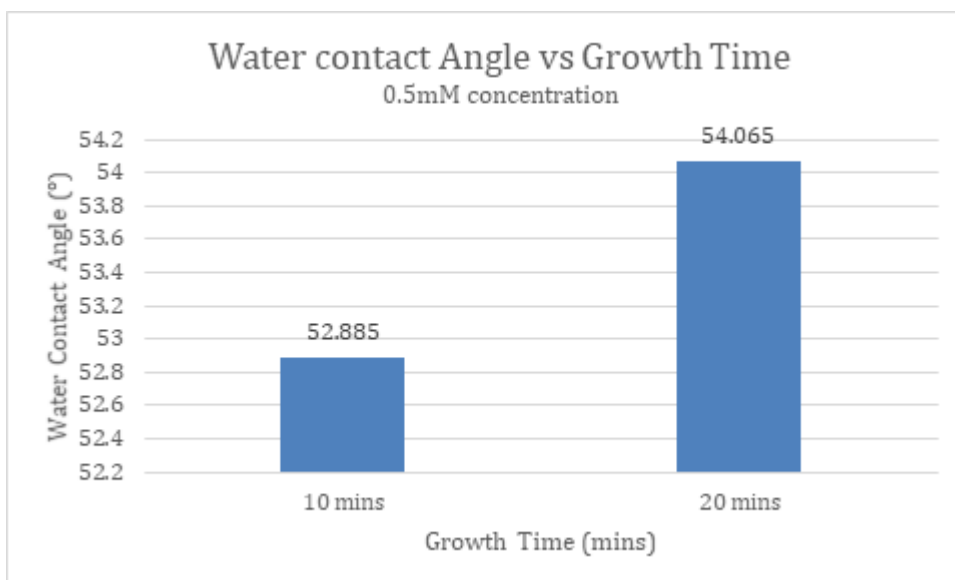


Figure 4.4: Graphical representation for Water contact angle obtained at various Growth durations of nanorods grown with a concentration of 0.5mM

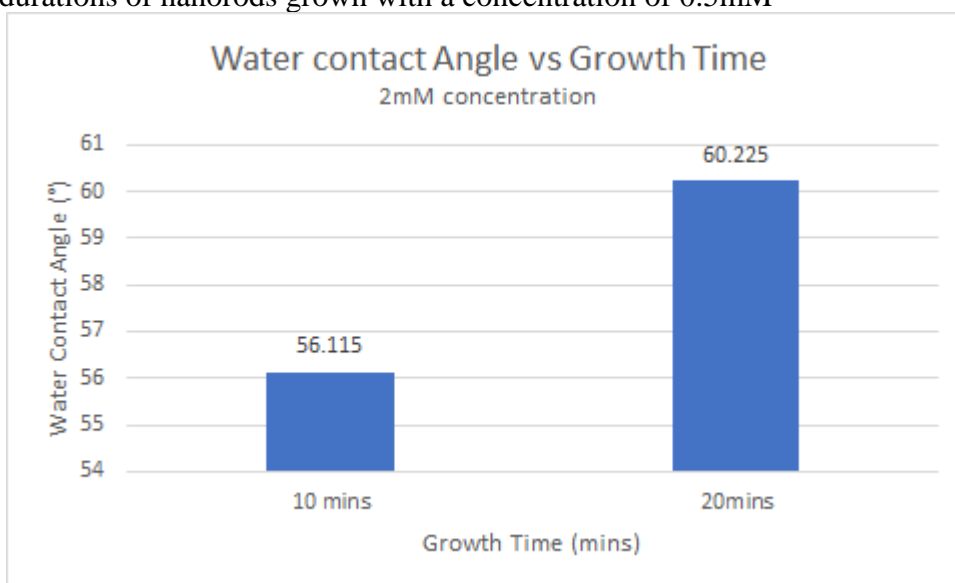


Figure 4.5: Graphical representation for Water contact angle obtained at various Growth durations of Nanorods grown with a concentration of 2 mM

From the above graphs in figure 4.4 and figure 4.5, we get to observe the surface structure of the samples. The parameter observed in these graphs is the water contact angle to the surface of the sample. The water contact angle mainly depends upon the surface roughness. As the growth duration increases, the number of nanorods formed increases, resulting in a high surface roughness. Due to which the water droplet doesn't spread much on the surface. So as a result, the water contact angle has been increasing with every increase in the growth duration as well as the growth concentration. The highest contact angle has been achieved for the growth concentration 2mM at the growth duration of 20mins.

4.2.2 Transmission Results:

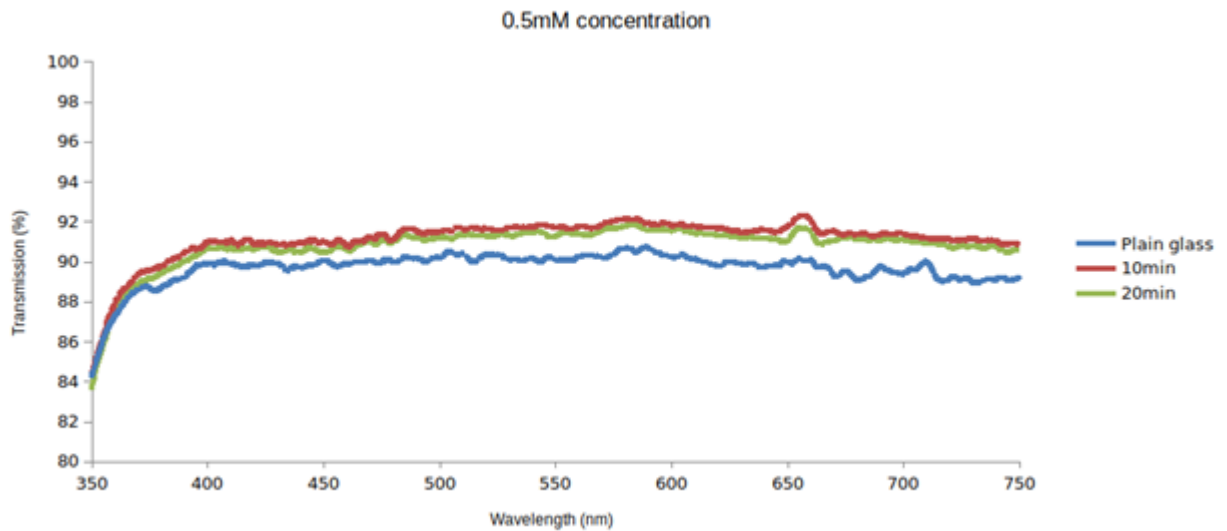


Figure 4.6: Transmission comparison between plain and coated samples generated for the growth concentration of 0.5mM and at a growth duration of both 10 mins and 20 mins

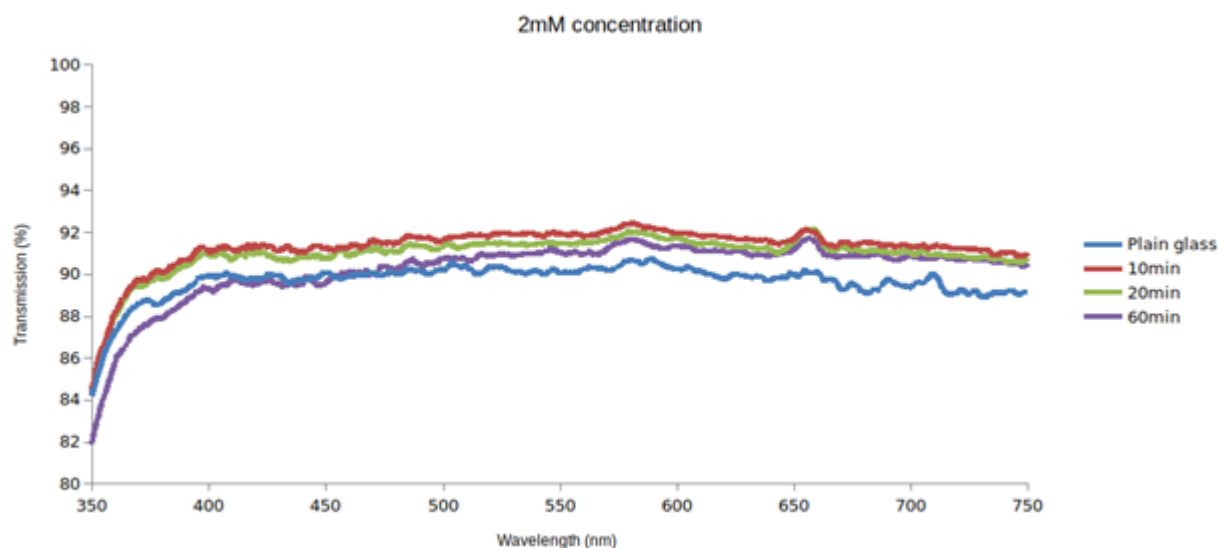


Figure 4.7: Transmission comparison between plain and coated samples generated for the growth concentration of 2mM and at a growth duration of 10 mins, 20 mins and 60 mins. All the samples depicted in the above graph were produced for growth concentrations of 0.5mM and 2mM at the growth durations of 10 mins, 20 mins and 60 mins.

We can clearly observe from the above graph that the anti-reflective coating produced has achieved the desired values. The transmission has been steadily decreasing for an increase in the growth duration. The maximum value of transmission was obtained for the sample with a growth duration of 10 mins. The samples (at both the concentrations of 0.5mM and 2mM) with growth durations of 10 mins, 20 mins and 60 mins have achieved a transmission greater than that of the plain glass. But, the transmission values for 60 mins is less when compared to that of 10 mins and 20 mins in both the graphs. The reason being that, as the growth duration increases, the roughness of the surface increases to an extreme value, resulting in less transmission values. In order to obtain high transmission values, we have to maintain the surface roughness at a moderate level.

The reflection at a surface depends upon the difference between the refractive indices of the two mediums through which the light is travelling. The greater the difference, the larger the reflection. If we can reduce this difference, the reflection can be automatically reduced. For instance, the refractive index of air is 1 and that of Silicon is 3.5. The nanorods layer which we prepared, when deposited on a silicon solar cell, can produce a refractive index just slightly more than that of air. The empty spaces between the nanorods are the main reason for the refractive index to be close to that of air (5%-10% above the refractive index of air). So that there won't be any abrupt changes in the refractive indices of the mediums. Hence, the reflection can be suppressed, and the efficiency of solar cell can be increased.

4.3 ZnO Nanocones

4.3.1 Scanning Electron Microscopy (SEM) Result

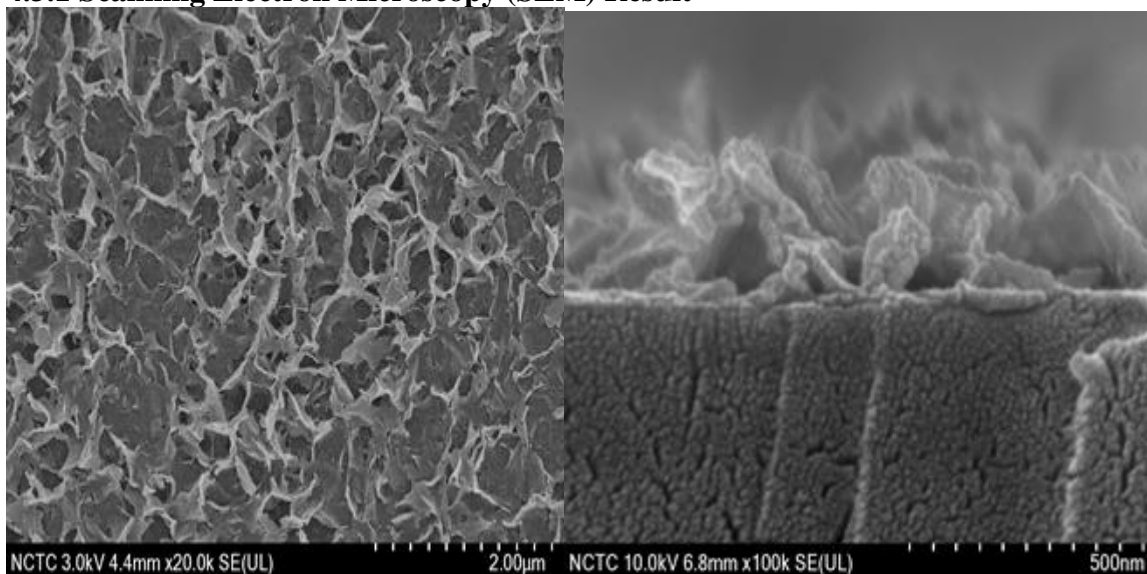


Figure 4.8: Images of nanocones grown for a growth duration of 30 mins, obtained from the test results of Scanning Electron Microscopy (SEM): (left)Top view 20k magnification, (right) Cross-sectional view 100k magnification

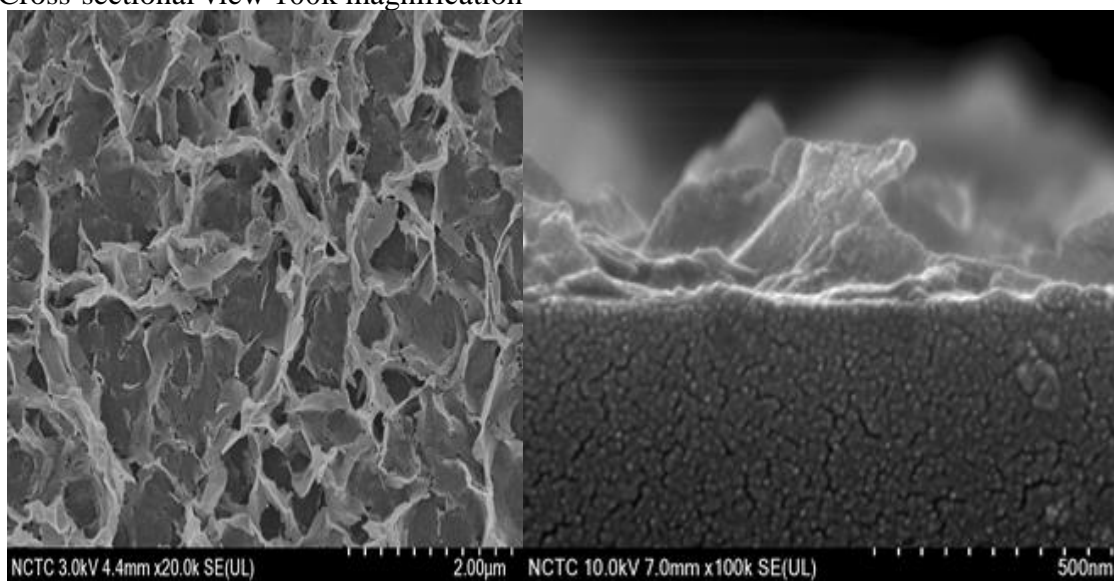


Figure 4.9: Images of nanocones grown for a growth duration of 60 mins, obtained from the test results of Scanning Electron Microscopy (SEM): (left)Top view 20k magnification, (right) Cross-sectional view 100k magnification

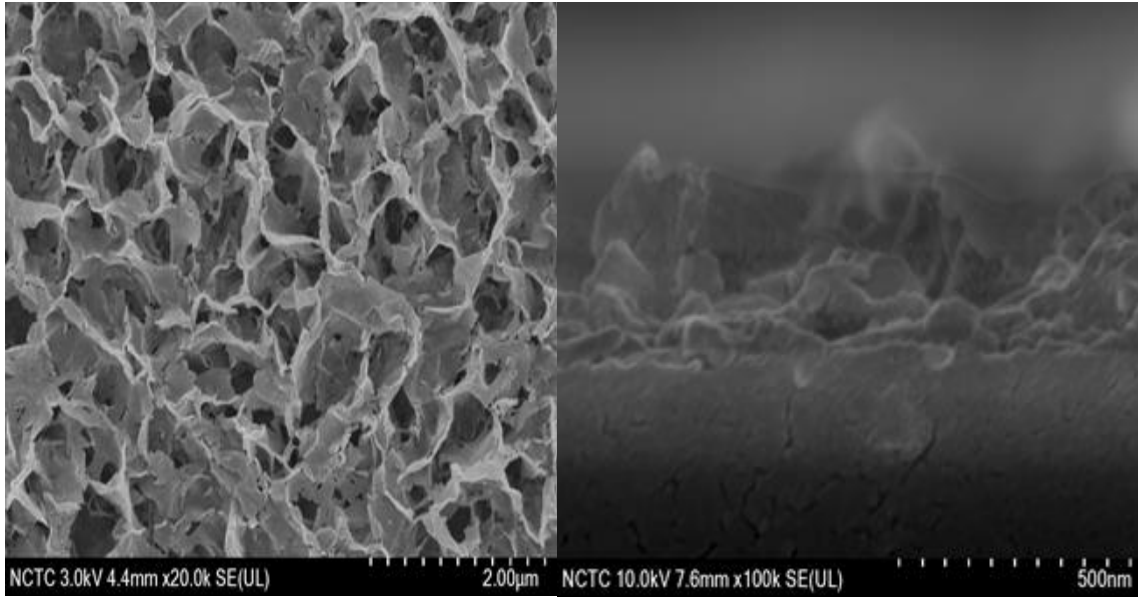


Figure 4.10: Images of nanocones grown for a growth duration of 180 mins, obtained from the test results of Scanning Electron Microscopy (SEM): (left)Top view 20k magnification, (right) Cross-sectional view 100k magnification

The above images from figure 4.8, figure 4.9 and figure 4.10 depict the images of SEM test for the generated Anti-reflective coating of nanocones for different growth durations of 30 mins, 1hr and 3hrs. The nanostructures (nanocones to be precise), have spread across the sample surface without much gaps in the between, resulting in good surface roughness. The size of the nanostructures can be observed to be steadily increasing. The gaps between the nanocones were also lessening as the growth duration was increased. Hence the roughness was increasing to an extreme level.

Avg_Length vs Growth time

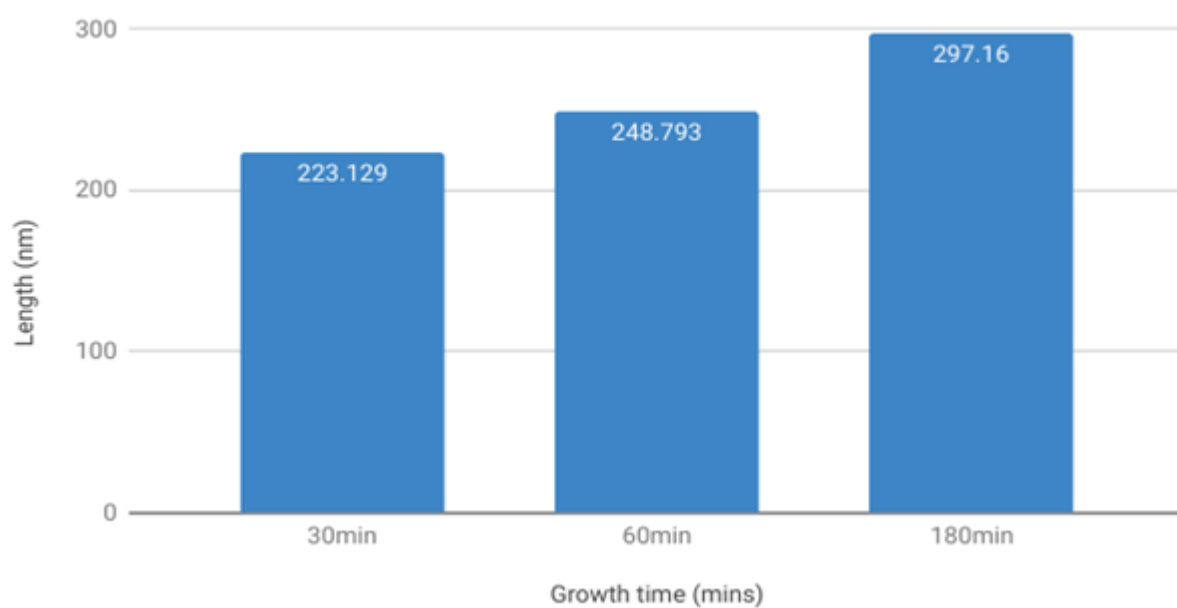


Figure 4.11: Graphical representation for Average length of Nanocones obtained at various Growth durations

Water Contact Angle vs Growth Time

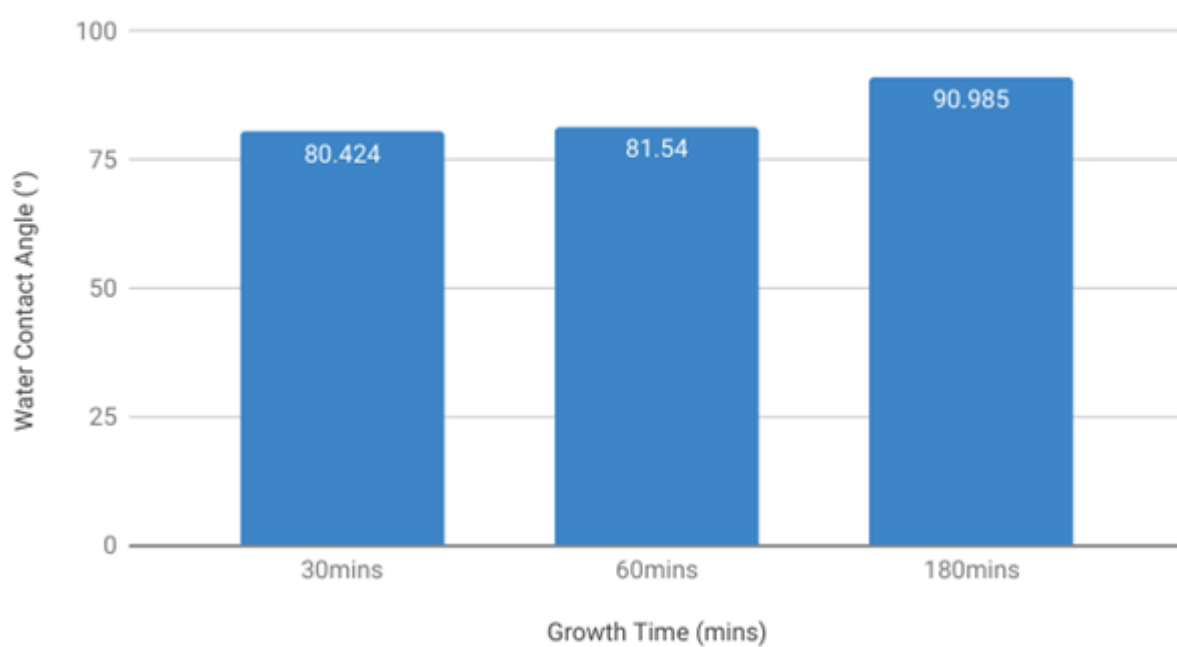


Figure 4.12: Graphical representation for Water contact angle obtained at various Growth durations of Nanocones

From the above graphs in figure 4.11 and figure 4.12, we get to observe the surface structure of the samples. From figure 4.11, we can observe that the length of the nanocones has increased with an increase of the growth duration. The maximum value was obtained for the growth duration of 180 mins. Another parameter observed was the water contact angle to the surface of the sample in figure 4.12. The water contact angle mainly depends upon the surface roughness. As the growth duration increases, the number of nanocones formed increases, resulting in a high surface roughness. Due to which the water droplet doesn't spread much on the surface. So as a result, the water contact angle has been increasing with every increase in the growth duration.

4.3.2 Transmission Results:

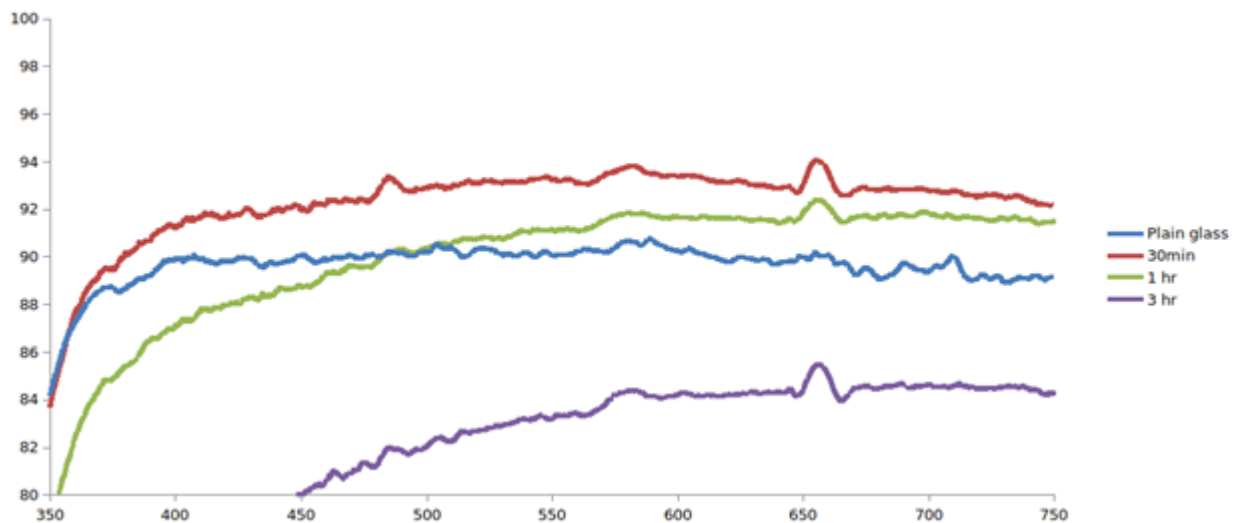


Figure 4.13: Transmission comparison between plain and coated samples generated at various growth durations

All the samples depicted in the above graph were produced by having the concentration of the seeded solution (1mM) and concentration of the growth solution (10mM) at a constant value and by varying only the growth duration (30 mins, 1hr and 3hrs).

We can clearly observe from the above graph that the anti-reflective coating produced has achieved the desired values. The transmission has been steadily decreasing for an increase in the growth duration. The maximum value of transmission was obtained for the sample with a growth duration of 30 mins. The samples with growth durations of both 30 mins and 1hr have achieved a transmission greater than that of the plain glass. Whereas, the sample with a growth of 3hrs has been observed to have transmission less than the plain glass. As the growth duration has been increasing, the roughness of the surface increases to an extreme value, resulting in less transmission values. In order to obtain high transmission values, we have to maintain the surface roughness at a moderate level.

CHAPTER 5

CONCLUSION

In this research study, I have defined and described the working of an Antireflective Coating. I have mentioned about its existing usage and future scope in the field of power electronics. Then, I have discussed about how the shape and size of nanostructures influence the surface morphology. I have produced two types of antireflective coatings: one with nanorods and the other with nanocones. Then, studied their performance based on transmission comparison between plain and coated samples. The surface structure was analyzed using the SEM results. The analysis was based on water contact angle and length of the nanostructures (nanorods and nanocones) grown. The results were clear that the antireflective coatings produced have achieved the desired values.

REFERENCES

1. Hajar Ghannam, Zakaria Oulad EI hmaidi, Zineb Yamlahi Alami, Mohamed Addou and Adil Chahboun, "Simulation of hydrophobic surfaces: A case study of ZnO thin film",
2. 2014 International Renewable and Sustainable Energy Conference (IRSEC) 2014
3. Sheng Yang, Yiting Wang, Xiangyu Zeng, Jia Zhou, "Fabrication and Analysis of Super- hydrophobic ZnO film for microfluidic devices", ICSICT-2010 - 2010 10th IEEE International Conference on Solid-State and Integrated Circuit Technology, Proceedings, 2010, pages: 1428-1430
4. Hanyang Gu , Chi Wang, Shengjie Gong, Yong Mei, Huang Li, Weimin Ma, "Investigation on contact angle measurement methods and wettability transition of porous surfaces" Surface and Coatings Technology, volume: 292, 2016, pages 72-77.
5. A. Nakajima, K Hashimoto and T.Watanabe, "Recent studies on superhydrophobic films," Monatshefte fur Chemie, vol. 132, pp. 31-41,1997.
6. Y. Hashimoto ; K. Mogi ; T. Yamamoto, "Release agent-free low-cost double transfer nanoimprint lithography for moth-eye structure", 16th International Conference on Nanotechnology - IEEE NANO 2016, 2016, issue:1, pages: 318-320
7. Corey S. Thompson, Min Zou, "Investigation of Moth-Eye Antireflection Coatings for Photovoltaic Cover Glass Using FDTD Modeling Method", 2014 IEEE 40th Photovoltaic Specialist Conference (PVSC), 2014,pages: 2273-2275
8. L. Yao and J. He, "Recent progress in anti-reflection and self-cleaning technology From surface engineering to functional surfaces," Prog. in Materials Science, vol. 61, pp. 94-143, 2014.
9. Y. C. Lee, C. C. Chang, and Y. Y. Chou, "Fabrication of broadband anti-reflective sub-micron structures using polystyrene sphere lithography on a Si substrate." Photon Nanostruct: Fundam Appl, (2013).
10. Q. Yang, X. A. Zhang, A. Bagal, W. Guo, and C. H. Chang, "Antireflection effects at nanostructured material interfaces and the suppression of thin-film interference," Nanotechnology, vol. 24, (2013).
11. M. Burghoorn, D. Roosen-Melson, J. de Riet, S. Sabik, Z. Vroon, I. Yakimets, and P.Buskens, "Single layer broadband anti-reflective coatings for plastic substrates produced by full wafer and roll-to-roll step-and-tlash nano-imprint lithography," Materials, vol. 6, pp. 3710-26, (2013).
12. Y. M. Song, Y. Jeong, C. I. Yeo, and Y. T. Lee, "Enhanced power generation in concentrated photovoltaics using broadband antireflective cover glasses with moth eye structures," Optics Express, vol. 20, no. 26, (2012).
13. Kelvii Wei GUO, "Surface Treatments as Moth eye Structures for a Broadband Anti-Reflective Layer" 06 August, 2016.volume:4
14. Yuki Hashimoto, Katsuo Mogi, Takatoki Yamamoto, "Fabrication Method of Moth-eye Using UV-curable Polydimethylsiloxane with Vitrification by Vacuum Ultraviolet Light", IEEE-NANO 2015 - 15th International Conference on Nanotechnology, 2015, pages: 128-131.
15. Cheng-Hsin Chuang, Deng-Maw Lu, Po-Hsiang Wang, "Fabrication of Antireflective Polymer Films with Subwavelength Structures using Roll to Roll Nanoimprint Lithography" Symposium on Design, Test, Integration and Packaging of MEMS/MOEMS, DTIP 2016, 2016, pages: 1-5.

16. Srikanth Ravipati, Fu-Hsiang Ko , Jiann Shieh , “PLASMA MADE ANTIREFLECTIVE GaAs NANOGRASS”, 2012 Abstracts IEEE International Conference on Plasma Science, pages: 2221
17. Christoph Morhard, Claudia Pacholski, Robert Brunner, Michael Helgert, Dennis Lehr, Joachim Spatz, “Antireflective ‘moth-eye’ structures fabricated by a cheap and versatile process on various optical elements”, August 15-18, 2011.
18. Liang Gu , Yanyan Wang , Chengyun Xu , “Construction of Superhydrophobic Surfaces by Solgel Techniques” Conference Program Digest - 7th International Conference on Manipulation, Manufacturing and Measurement on the Nanoscale, IEEE 3M-NANO 2017,2018,volume: 2018-Janua,pages: 156-160.
19. Yu Zeng , XiFang Chen , Zao Yi , Yougen Yi , Xibin Xu “Fabrication of p-n heterostructure ZnO/Si moth-eye structures: Antireflection, enhanced charge separation and photocatalytic properties”, Applied Surface Science, 2018,volume: 441,pages: 40-48
20. Beom-Ki Shin , Tae-ILee , JunjieXiong , ChanghunHwang , GapseongNoh , Joong Hwee Cho , Jae-MinMyoung “BottomgrownZnOnanorodsforanantireflectivemoth-eye structure onCuInGaSe2 solar cells” Solar Energy Materials and Solar Cells, 2011,volume: 95,issue:9,pages: 2650-2654.
21. Qinghui Mua, Yaogang Li, Hongzhi Wang, Qinghong Zhang, “Self-organized TiO2 nanorod arrays on glass substrate for self-cleaning antireflection coatings” Journal of Colloid and Interface Science, 2012, volume: 365, issue:1, pages: 308-313.
22. Liang Zhang, Changli Lü, Yunfeng Li, Zhe Lin, Zhanhua Wang, Heping Dong Tieqiang Wanga, Xuemin Zhang a, Xiao Li a, Junhu Zhang a, Bai Yang “Fabrication of biomimetic high performance antireflective and antifogging film by spin-coating” Journal of Colloid and Interface Science, 2012, volume: 374, issue:1, pages: 89-95.
23. Yanjing Tuo, Weiping Chen, Haifeng Zhang, Pujun Li, Xiaowei Liu” One-step hydrothermal method to fabricate drag reduction superhydrophobic surface on aluminum foil” Applied Surface Science, 2018volume: 446, pages: 230-235
24. Arun D Rao, Suresh Karalatti, Tiju Thomas and Praveen C Ramamurthy,” Organic solar cell by using vertically aligned nanostructured ZnO nanorods” 2013 IEEE 39th Photovoltaic Specialists Conference (PVSC), 2013, pages: 2752-2756.
25. K. Kawano, R. Pacios, D. Poplavskyy, J. Nelson, D. D. C. Bradley, and J. R. Durrant, “Degradation of organic solar cells due to air exposure,” Solar Energy Materials and Solar Cells, vol. 90, no. 20, pp. 3520–3530, Dec. 2006
26. W. I. Park, J. S. Kim, G.-C. Yi, M. H. Bae, and H.-J. Lee, “Fabrication and electrical characteristics of high-performance ZnO nanorod field-effect transistors,” Applied Physics Letters, vol. 85, no. 21, pp. 5052–5054, Nov. 2004.
27. A. I. Hochbaum and P. Yang, “Semiconductor Nanowires for Energy Conversion,” Chem. Rev., vol. 110, no. 1, pp. 527–546, Jan. 2010
28. S.-L. Zhao, P.-Z. Kan, Z. Xu, C. Kong, D.-W. Wang, Y. Yan, and Y.-S. Wang, “Electroluminescence of ZnO nanorods/MEH-PPV heterostructure devices,” Organic Electronics, vol. 11, no. 5, pp. 789–793, May 2010.
29. Muhammad Quisar Lokman, Hazli Rafis Bin Abdul Rahim, Sulaiman Wadi Harun, G. Louis Hornyak, Waleed Soliman Mohammed, “Light backscattering (e.g. reflectance) by ZnO nanorods on tips of plastic optical fibres with application for humidity and alcohol vapour sensing” Micro & Nano Letters, 2016, volume: 11, issue: 12, pages: 832-836.

30. Wan-Hsuan Tsai and Shih-Shou Lo, "The Influence on Intensity Ratio of Peak Emission between Recombination of Free-Excitons and Deep-Defect for ZnO Nanostructure Evolution from Nanorods to Nanotubes", 16th International Conference on Nanotechnology - IEEE NANO 2016, 2016, pages: 387-389
31. Shuwang Duo, Ruifang Zhong, Zhao Liu, Jun Wang, Tingzhi Liu, Chenlian Huang, Haoshuang Wu, "One-step hydrothermal synthesis of ZnO microflowers and their composition-/hollow nanorod-dependent wettability and photocatalytic property" *Journal of Physics and Chemistry of Solids*, 2018, volume: 120, issue: April, pages: 20-33.
32. C. Lian, X.Y. Zhong Wang, One-step approach to the growth of ZnO nano /microrods on cellulose toward its durable superhydrophobicity, *Adv. Mater. Interfaces* 4 (2017) 1700550.
33. Jianguo Lv , Pengpeng Yan , Min Zhao , Yue Sun , Fengjiao Shang , Gang He Miao Zhang, Zhaoqi Sun, "Effect of ammonia on morphology, wettability and photoresponse of ZnO nanorods grown by hydrothermal method", *Journal of Alloys and Compounds*, 2015, volume: 648, pages: 676-680.
34. Chen-Chen Chung, Kung-Liang Lin, Hung-Wei Yu, Nguyen-Hong Quan, Chang-Fu Dee and Edward Yi Chang, "Hydrothermal growth of ZnO nanotubes on InGaP/GaAs/Ge Solar Cells", *IEEE International Conference on Semiconductor Electronics, Proceedings, ICSE*, 2014, pages: 517-520.
35. A. Luque, A. Marti, and A.J. Nozik: *MRS Bull.* 32, 236 (2007).
36. Chung-Wen Lan, "Enhancing Performance of ZnO Dye-sensitized Solar Cells by Incorporation of Multiwalled Carbon Nanotubes", *Nanoscale Research Letters*, 2012, volume: 7, issue: 1, pages: 166.
37. C. Liu, et al., *Carbon*, Vol. 47, 2009, pp. 1158.
38. W. Zhu, C. Bower, G.P. Kochanski, and S. Jin, *Solid State Electron.* Vol. 45, 2001, pp. 921.
39. Q. Zhang, et al., *Adv. Mater. ACS Applied Materials and Interfaces*, 2015, Vol. 21, 2009, pp. 6706-6715
40. Paul Glatkowski, Evgeniya Turevskaya, David Britz, David Rich, Matt DiCologero, Timothy Kellher, John Sennott, David Landis, Robert Braden, Patrick Mack, Joseph Pichel "CARBON NANOTUBE TRANSPARENT ELECTRODES: A CASE FOR PHOTOVOLTAICS" *Carbon*, 2009, pages: 1302-1305
41. K. Lee, Z. Wu, Z. Chen, F. Ren, S. J. Pearton, and A. G. Rinzler, "Single Wall Carbon Nanotubes for p-Type Ohmic Contacts to GaN Light-Emitting Diodes," *Carbon*, 4, 2004, pages: 911-914.
42. Nadia Abdel Aal, Faten Al-Hazmi, Ahmed A. Al-Ghamdi, Attieh A Al-Ghamdi, Farid El-Tantawy, F. Yakuphanoglu, "Novel rapid synthesis of zinc oxide nanotubes via hydrothermal technique and antibacterial properties", *Volume 135*, 25 January 2015, Pages 871-877.
43. Sze-Mun Lam, Jin-Chung Sin, Ahmad Zuhairi Abdullah, Abdul Rahman Mohamed, "Green hydrothermal synthesis of ZnO nanotubes for photocatalytic degradation of methylparaben", *December Materials Letters*, 2013, volume: 93, pages: 423-426
44. Nuengruethai Ekthammathat, Titipun Thongtem, Anukorn Phuruangrat, Somchai Thongtem, "Characterization of ZnO flowers of hexagonal prisms with planar and hexagonal pyramid tips grown on Zn substrates by a hydrothermal process", *Superlattices and Microstructures*, 2013 volume: 53, issue: 1, pages: 195-203.